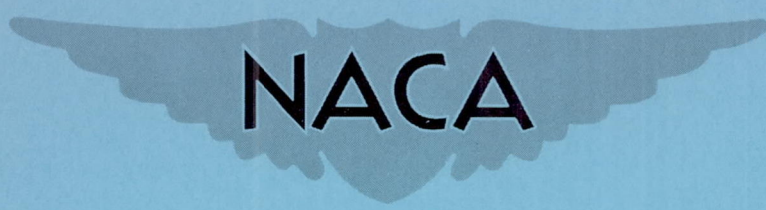


CONFIDENTIAL

NACA RM L54F25



RESEARCH MEMORANDUM

EFFECTS OF CANOPY, REVISED VERTICAL TAIL, AND A YAW-DAMPER
VANE ON THE AERODYNAMIC CHARACTERISTICS OF A 1/16-SCALE
MODEL OF THE DOUGLAS D-558-II RESEARCH AIRPLANE

AT A MACH NUMBER OF 2.01

By Ross B. Robinson

Langley Aeronautical Laboratory
Langley Field, Va.

CLASSIFICATION CHANGED TO UNCLASSIFIED
AUTHORITY: NACA RESEARCH ABSTRACT NO. 128
EFFECTIVE DATE: JUNE 24, 1958
WHL

CLASSIFIED DOCUMENT

This material contains information affecting the National Defense of the United States within the meaning of the espionage laws, Title 18, U.S.C., Secs. 793 and 794, the transmission or revelation of which in any manner to an unauthorized person is prohibited by law.

NATIONAL ADVISORY COMMITTEE FOR AERONAUTICS

WASHINGTON

August 30, 1954

CONFIDENTIAL

NATIONAL ADVISORY COMMITTEE FOR AERONAUTICS

RESEARCH MEMORANDUM

EFFECTS OF CANOPY, REVISED VERTICAL TAIL, AND A YAW-DAMPER
VANE ON THE AERODYNAMIC CHARACTERISTICS OF A 1/16-SCALE
MODEL OF THE DOUGLAS D-558-II RESEARCH AIRPLANE
AT A MACH NUMBER OF 2.01

By Ross B. Robinson

SUMMARY

The aerodynamic characteristics in pitch and sideslip of a revised 1/16-scale model of the Douglas D-558-II research airplane, with and without a yaw-damper vane, are presented for a Mach number of 2.01. The revised model incorporated a canopy and a modified vertical tail in order to simulate more closely the present airplane configuration. The model was tested through an angle-of-attack range of -2° to about 13° at an angle of sideslip of 0° and an angle-of-sideslip range of -2° to about 10° at an angle of attack of 0° . The results are compared with those previously obtained for the original model configuration.

The revised configuration had higher directional stability, trim lift coefficients, and drag and more positive effective dihedral than the original configuration. The static longitudinal stability, the lift-curve slope, and the effectiveness of the horizontal stabilizer were not significantly altered by the changes in configuration.

The vane effectiveness parameter $C_{n\delta_V}$ increased rapidly with increasing lift coefficient and but only slightly with angle of sideslip.

INTRODUCTION

Various investigations have been conducted that are concerned with the aerodynamic characteristics of the Douglas D-558-II research airplane which is currently undergoing flight tests by the NACA High-Speed Flight Research Station at Edwards Air Force Base, Calif. A 1/16-scale model of the original configuration has been investigated at high subsonic and low supersonic speeds in the Langley 8-foot high-speed tunnel (ref. 1)

and at Mach numbers of 1.61 and 2.01 in the Langley 4- by 4-foot supersonic pressure tunnel (refs. 2 and 3). Recently the original model has been modified to simulate more closely the present airplane configuration by the addition of a canopy and by increasing the size of the vertical tail. A small vane simulating that to be used in conjunction with a yaw damping system proposed by the Stability Analysis Section of the Langley Aeronautical Laboratory (ref. 4) was also incorporated into the model.

The present paper presents the aerodynamic characteristics of the revised model in pitch and sideslip, with and without a yaw-damper vane, at a Mach number of 2.01 and a Reynolds number of 1.46×10^6 based on the wing mean aerodynamic chord. The model was tested through an angle-of-attack range of about -2° to about 13° at an angle of sideslip of 0° and an angle-of-sideslip range of -2° to about 10° at an angle of attack of 0° . These results are compared with those obtained for the original model configuration.

COEFFICIENTS AND SYMBOLS

The results of the investigation are presented as standard NACA coefficients of forces and moments. The data are referred to the stability axis system (fig. 1) with the reference center of gravity at 25 percent of the wing mean aerodynamic chord. The coefficients and symbols are defined as follows:

C_L	lift coefficient, $-Z/qS$
C_X	longitudinal-force coefficient, X/qS
C_m	pitching-moment coefficient, $M'/qS\bar{c}$
C_Y	lateral-force coefficient, Y/qS
C_l	rolling-moment coefficient, L/qSb
C_n	yawing-moment coefficient, N/qSb
X	force along X-axis
Y	force along Y-axis
Z	force along Z-axis
L	moment about X-axis
M'	moment about Y-axis

N	moment about Z-axis
q	free-stream dynamic pressure
b	wing span
S	total wing area including body intercept
\bar{c}	wing mean aerodynamic chord, 5.46 in.
M	Mach number
α	angle of attack of body center line, deg
β	angle of sideslip of body center line, deg
i_t	stabilizer incidence angle with respect to body center line, deg
δ_r	rudder deflection with respect to body center line, deg
δ_v	yaw-damper vane angle with respect to body center line, deg
L/D	lift-drag ratio, $C_L/-C_X$ for $\beta = 0^\circ$
$C_{L\alpha}$	lift-curve slope, $dC_L/d\alpha$
C_{mC_L}	static-longitudinal-stability derivative, dC_m/dC_L
$\frac{\Delta C_m}{\Delta i_t}$	incremental change in pitching-moment coefficient with stabilizer incidence
$C_{Y\beta} = dC_Y/d\beta$	
$C_{n\beta}$	static-directional-stability derivative, $dC_n/d\beta$
$C_{l\beta}$	effective-dihedral parameter, $dC_l/d\beta$
$C_{n\delta_v} = dC_n/d\delta_v$	
$C_{Y\delta_v} = dC_Y/d\delta_v$	
$C_{l\delta_v} = dC_l/d\delta_v$	
$(\Delta C_Y)_t$	increment of lateral-force coefficient due to addition of vertical tail

- $(\Delta C_n)_t$ increment of yawing-moment coefficient due to addition of vertical tail
- $(\Delta C_l)_t$ increment of rolling-moment coefficient due to addition of vertical tail

MODEL AND APPARATUS

A three-view drawing of the model is presented in figure 2. Details of the yaw-damper vane are shown in figure 3. The vane is offset from the center line of the body so that clearance may be provided for nose-wheel retraction on the airplane. The modifications to the original model are: (1) addition of a canopy and (2) alteration of the vertical tail to a plan form similar to that now used on the airplane (see fig. 2). The afterportion of the fuselage was slightly enlarged on both models to accommodate the balance. Geometric characteristics of the model are presented in table I. Coordinates for the body are given in table II and for the canopy in table III.

The model was equipped with a wing having 35° of sweep of the 0.30-chord line of the unswept panel, aspect ratio 3.57, taper ratio 0.565, and NACA 63-010 airfoil sections normal to the 0.30-chord line. The wing had 3° of incidence with respect to the fuselage center line and 3° of negative geometric dihedral. The model wing section differs from that of the airplane in that the wing tip section of the airplane is an NACA 63₁-012 airfoil section.

Deflections of the stabilizer and yaw-damper vane were set manually. The rudder deflection was 0° for the present investigation. The canopy, vane, wing, vertical tail, and stabilizer were removable to facilitate the investigation of various combinations of component parts.

Force and moment measurements were made through the use of a six-component internal strain-gage balance. Base pressure was measured by a single tube in the plane of the model base.

TEST CONDITIONS

The conditions for the tests were:

Mach number	2.01
Reynolds number, based on \bar{c}	1.46×10^6
Stagnation dewpoint, $^\circ\text{F}$	-25
Stagnation pressure, lb/sq in. abs	13

Stagnation temperature, °F	100
Mach number variation	±0.015
Flow angle in horizontal or vertical plane, deg	±0.1

CORRECTIONS AND ACCURACY

The angles of attack and sideslip were corrected for the deflection of the balance and sting under load. No corrections were applied to the data to account for the tunnel flow variations. The base pressure was measured and the longitudinal force data were corrected to a base pressure equal to the free-stream static pressure.

The estimated errors in the data are:

C_L	±0.004
C_X	±0.002
C_Y	±0.002
C_m	±0.0007
C_n	±0.0005
C_l	±0.0003
α , deg	±0.1
i_t , deg	±0.1
δ , deg	±0.1

PRESENTATION OF RESULTS

The results of this investigation are presented in two sections: (1) the effects of the canopy and revised vertical tail on the aerodynamic characteristics of the model and (2) the characteristics of the yaw-damper vane in pitch and sideslip and the effects of the vane on the characteristics of the revised model. A table of the figures presenting the results is given below:

	<u>Figure</u>
Effects of canopy and revised vertical tail on the aerodynamic characteristics in pitch, $\beta = 0^\circ$	4
Effects of canopy and revised vertical tail on the aerodynamic characteristics in sideslip, $\alpha = 0^\circ$	5
Effects of canopy and revised vertical tail on incremental lateral characteristics produced by vertical tail, $\alpha = 0^\circ$	6

Variation of $C_{n\beta}$ with Mach number	7
Effects of yaw-damper vane on the aerodynamic characteristics in pitch, $\beta = 0^\circ$ and $i_t = 0^\circ$	8
Effects of yaw-damper-vane deflection on the aerodynamic characteristics in sideslip, $\alpha = 0^\circ$ and $i_t = 0^\circ$	9
Variation of lateral characteristics with yaw-damper-vane deflection for various values of C_L	10
Summary of yaw-damper-vane characteristics	11

The model with the canopy and the revised vertical tail used in this investigation is designated the revised model; the model without the canopy and with the original vertical tail is referred to as the original model (refs. 2 and 3).

A summary of static longitudinal and lateral stability characteristics for the various configurations without the yaw-damper vane are presented in table IV. Experimental and estimated yaw-damper-vane characteristics are given in table V.

DISCUSSION

Effects of Canopy and Revised Vertical Tail

Aerodynamic characteristics in pitch.- Addition of the canopy and revised vertical tail resulted in about 10 percent greater values of longitudinal force for the revised model in the low lift range but did not significantly alter the lift-curve slope $C_{L\alpha}$ or the static longitudinal stability (fig. 4 and table IV). Most of the increased longitudinal force and the positive increase in lift at constant angle of attack is produced by the canopy (figs. 4 and 5(b)). The lift on the canopy and the greater drag of the larger vertical tail produce more positive values of C_m at constant lift coefficients for the revised model, with a resulting increase in trim lift coefficient for both values of i_t . For constant angles of attack the stabilizer effectiveness $\frac{\Delta C_m}{\Delta i_t}$ was about the same for both models (table IV).

Aerodynamic characteristics in sideslip.- The canopy had a destabilizing effect on the directional-stability derivative as expected and increased the effective dihedral (fig. 5). The effect of the revised vertical tail was to increase both the directional-stability derivative and the positive effective dihedral of the complete model (fig. 5 and table IV). The increases in incremental lateral characteristics produced by the larger vertical tail in conjunction with the canopy (see fig. 6)

are approximately proportional to the increased tail area. The value of $C_{n\beta}$ was nearer to that estimated for the complete airplane in reference 5 (fig. 7).

Little change in the variation of the longitudinal characteristics with sideslip angle was obtained for any of the configurations tested (fig. 5(b)).

It should be pointed out that the value of i_t was 0° for the revised model and 2° for the original model, but this small difference should have little effect on the variation of the aerodynamic characteristics with sideslip.

Effects of Yaw-Damper Vane

Aerodynamic characteristics in pitch.- The yaw-damper vane produced a significant positive increment in C_m which increased with positive deflection of the vane (fig. 8), probably as a result of more positive pressures under the nose and wake effects on the lifting surfaces. As a result, trim lift coefficients also increased with vane deflection. The effectiveness of the vane in producing C_n increased greatly with increasing C_L (figs. 8 and 10), whereas the values of C_l and C_y for a given deflection varied little with lift coefficient.

Aerodynamic characteristics in sideslip.- The vane decreased the directional stability $C_{n\beta}$ from a value of 0.0024 to 0.0020 and slightly increased the positive effective dihedral of the model (fig. 9 and table V). The experimental incremental change in the slope of the lateral-force coefficient-curves $\Delta C_{Y\beta}$ due to the vane agreed well with the value estimated by the method of reference 6 (table V). Values of $\Delta C_{l\beta}$ and $\Delta C_{n\beta}$ estimated in a similar manner are somewhat low. For the range of sideslip angles investigated, the changes in the values of C_L , C_X , and C_m at a constant vane deflection were slight. Experimental values of $C_{Y\delta_V}$, $C_{l\delta_V}$, and $C_{n\delta_V}$ obtained from figure 10 were close to those estimated by the method of reference 7 considering the vane to be an isolated lifting surface (table V). The vane effectiveness parameter $C_{n\delta_V}$ increased rapidly with increasing lift coefficient and slightly with angle of sideslip (fig. 11). The dashed portion of the β_{trim} curve was estimated by using a value of $C_{n\delta_V}$ for $\alpha = 0^\circ$ to extrapolate to a vane deflection of 15° . Since the vane is not symmetrically mounted on the fuselage, a vane deflection of -4° or a rudder deflection of about -1.5° (ref. 3) would be required to maintain zero sideslip. The rudder was about three times as effective as the vane in producing trim sideslip angles.

CONCLUSIONS

A wind-tunnel investigation has been made with the revised 1/16-scale model of the Douglas D-558-II research airplane incorporating a canopy and a modified vertical tail to simulate more closely the present airplane and a fuselage-mounted yaw-damper vane. The results of this investigation at a Mach number of 2.01 indicated the following conclusions:

1. The revised configuration compared to the original configuration indicated higher directional stability, positive effective dihedral, trim lift coefficients, and drag. The static longitudinal stability, the lift-curve slope, and the effectiveness of the horizontal stabilizer were not significantly altered.

2. The vane effectiveness parameter $C_{n\delta_V}$ increased rapidly with increasing lift coefficient and slightly with angle of sideslip.

3. The unsymmetrical location of the vane on the fuselage required slight rudder or vane deflections to maintain zero sideslip.

4. Moderate increases in positive pitching-moment coefficient and higher values of trim lift coefficient resulted from deflection of the vane.

Langley Aeronautical Laboratory,
National Advisory Committee for Aeronautics,
Langley Field, Va., June 16, 1954.

REFERENCES

1. Osborne, Robert S.: High-Speed Wind-Tunnel Investigation of the Longitudinal Stability and Control Characteristics of a $\frac{1}{16}$ -Scale Model of the D-558-2 Research Airplane at High Subsonic Mach Numbers and at a Mach Number of 1.2. NACA RM L9C04, 1949.
2. Spearman, M. Leroy: Static Longitudinal Stability and Control Characteristics of a 1/16-Scale Model of the Douglas D-558-II Research Airplane at Mach Numbers of 1.61 and 2.01. NACA RM L53I22, 1953.
3. Grant, Frederick C., and Robinson, Ross B.: Static Lateral Stability Characteristics of a 1/16-Scale Model of the Douglas D-558-II Research Airplane at Mach Numbers of 1.61 and 2.01. NACA RM L53I29a, 1953.
4. Gates, Ordway B., Jr., Schy, Albert A., and Woodling, C. H.: An Analysis of the Lateral Stability of the Douglas D558-II Airplane Equipped With a Yaw Damper, With Special Reference to the Effect of Yaw-Damper Rate-Gyro Spin-Axis Orientation. NACA RM L52K14a, 1953.
5. Queijo, M. J., and Goodman, Alex: Calculations of the Dynamic Lateral Stability Characteristics of the Douglas D-558-II Airplane in High-Speed Flight for Various Wing Loadings and Altitudes. NACA RM L50H16a, 1950.
6. Nielsen, Jack N., and Kaattari, George E.: Method for Estimating Lift Interference of Wing-Body Combinations at Supersonic Speeds. NACA RM A51J04, 1951.
7. Piland, Robert O.: Summary of the Theoretical Lift, Damping-In-Roll, and Center-of-Pressure Characteristics of Various Wing Plan Forms at Supersonic Speeds. NACA TN 1977, 1949.

TABLE I

DIMENSIONS OF THE 1/16-SCALE MODEL OF THE DOUGLAS D-558-II RESEARCH AIRPLANE

Wing:

Root airfoil section (normal to 0.30 chord of unswept panel)	NACA 63-010
Tip airfoil section (normal to 0.30 chord of unswept panel)	NACA 63-010
Total area (including fuselage intercept), sq ft	0.684
Span, in.	18.72
Mean aerodynamic chord, in.	5.46
Root chord (parallel to plane of symmetry), in.	6.78
Tip chord (parallel to plane of symmetry), in.	3.83
Taper ratio	0.565
Aspect ratio	3.57
Sweep of 0.30-chord line of unswept panel, deg	35
Incidence at fuselage center line, deg	3
Dihedral, deg	-3
Geometric twist, deg	0

Horizontal tail:

Root airfoil section (normal to 0.30 chord of unswept panel)	NACA 63-010
Tip airfoil section (normal to 0.30 chord of unswept panel)	NACA 63-010
Area (including fuselage intercept), sq ft	0.156
Span, in.	8.98
Mean aerodynamic chord, in.	2.61
Root chord (parallel to plane of symmetry), in.	3.35
Tip chord (parallel to plane of symmetry), in.	1.68
Taper ratio	0.50
Aspect ratio	3.59
Sweep of 0.30-chord line of unswept panel, deg	40
Dihedral, deg	0
Elevator area, sq ft	0.059

Vertical tail:

Airfoil section (parallel to fuselage center line)	NACA 63-010
Area (leading edge and trailing edge extended to fuselage center line), sq ft	0.215
Span (from fuselage center line), in.	5.25
Root chord (parallel to fuselage center line), in.	9.14
Tip chord (parallel to fuselage center line), in.	1.67
Sweep of 0.30-chord line of unswept panel, deg	49
Rudder area, sq ft	0.030

Fuselage:

Length, in.	31.50
Maximum diameter, in.	3.75
Base diameter, in.	1.56
Fineness ratio	8.40

Yaw-damper vane:

Airfoil section	Double wedge
Span, in.	1
Taper ratio	0.5
Root chord, in.	2
Tip chord, in.	1
Aspect ratio	0.67

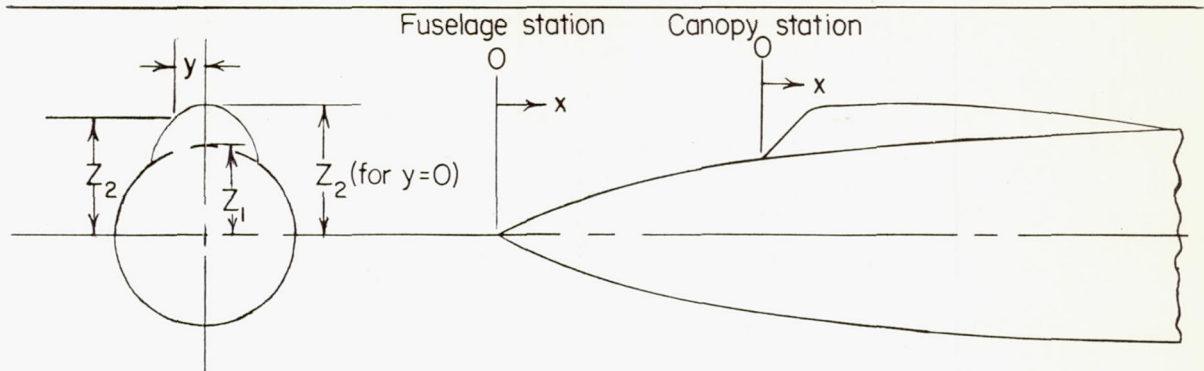
TABLE II

COORDINATES OF THE BODY

[x is distance along model center line from the nose of the model; r is the radius; all dimensions in inches]

x	r
0	0
1.000	.382
2.000	.719
3.000	1.010
4.000	1.256
5.000	1.457
6.000	1.614
7.000	1.729
8.000	1.806
9.000	1.851
10.000	1.871
11.000	1.875
16.250	1.875
17.000	1.872
18.000	1.858
19.000	1.833
20.000	1.794
21.000	1.743
22.000	1.679
23.000	1.602
24.000	1.513
24.297	1.485
31.500	.780

TABLE III
CANOPY ORDINATES



[All dimensions in inches]

Fuselage station, x	Canopy station, x_c	Canopy	
		Lower surface, Z_1	Upper surface, Z_2
3.38	0	1.109	1.109
3.44	.06	1.125	1.146
3.75	.37	1.199	1.371
4.06	.68	1.271	1.601
4.38	1.00	1.339	1.810
4.69	1.31	1.400	1.919
^a 5.31	1.93	1.516	2.020
^a 6.25	2.87	1.651	2.070
7.50	4.12	1.780	2.060
8.44	5.06	1.835	2.020
9.36	5.98	1.870	1.965
9.70	6.32	1.871	1.940
10.00	6.62	1.879	1.910
10.31	6.93	1.880	1.880
10.61	7.23	1.882	1.882

^aCross sections normal to plane of symmetry:

At $x_c = 1.93$

y	Z_2
0	2.020
±.25	1.969
±.50	1.582

At $x_c = 2.87$

y	Z_2
0	2.070
±.25	2.030
±.50	1.915
±.75	1.591

TABLE IV
SUMMARY OF THE AERODYNAMIC CHARACTERISTICS FOR
ORIGINAL AND REVISED MODELS

(a) Complete model

Model	$C_{L\alpha}$	C_{mCL}	$C_{X_{min}}$	$\frac{\Delta C_m}{\Delta i_t}$ ($\alpha = 6.5^\circ$)	$C_{L_{trim}}$ ($i_t = -6^\circ$)	α_{trim} ($i_t = -6^\circ$)	L/D_{trim} ($i_t = -6^\circ$)	$C_{Y\beta}$ ($\alpha = 0^\circ$)	$C_{l\beta}$ ($\alpha = 0^\circ$)	$C_{n\beta}$ ($\alpha = 0^\circ$)
Original model	0.047	-0.365	0.061	-0.018	0.425	8.8	2.95	-0.0125	-0.0014	0.0020
Revised model	.047	-.356	.067	-.018	.445	9.4	2.97	-.014	-.0019	.0024
Estimates for revised model from reference 5								-0.013	-0.0008	.0036

CONFIDENTIAL

(b) Tail off

Model	$C_{L\alpha}$	C_{mCL}	$C_{X_{min}}$	$C_{Y\beta}$	$C_{l\beta}$	$C_{n\beta}$
Original model	^a 0.0405	^a 0	^a 0.053	^b -0.0047	^b 0	^b -0.0036
Revised model ^c	.0425	0	.056	-.0053	0	-.0039

^aHorizontal tail off, no canopy

^bHorizontal and vertical tails off, no canopy

^cHorizontal and vertical tails off, with canopy

TABLE V

COMPARISON OF EXPERIMENTAL AND ESTIMATED
VANE CHARACTERISTICS

	$\Delta C_{Y\beta}$ (a)	$\Delta C_{l\beta}$ (a)	$\Delta C_{n\beta}$ (a)	$C_{Y\delta V}$	$C_{l\delta V}$	$C_{n\delta V}$
Experimental	-0.0020	-0.0002	-0.0004	-0.0008	0	0.00022
Estimated	-.0015	.00015	-.0007	-.0006	.00007	.00026

^aIncremental slopes $\Delta C_{Y\beta}$, $\Delta C_{l\beta}$, and $\Delta C_{n\beta}$ are changes in characteristics of complete configuration resulting from addition of the vane.

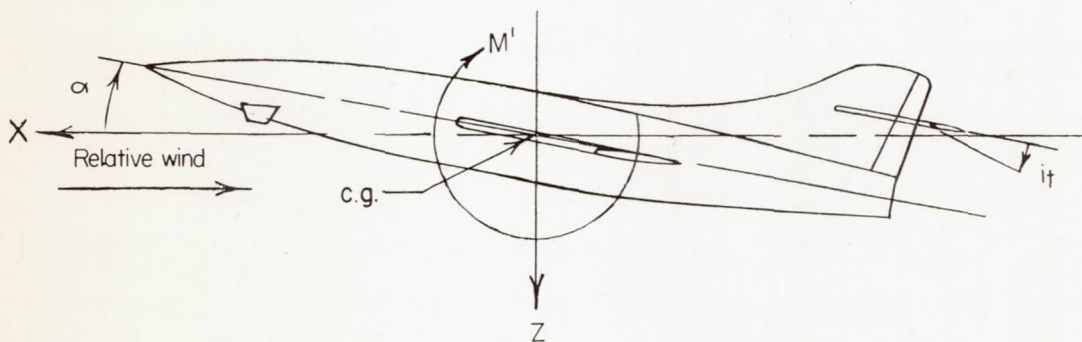
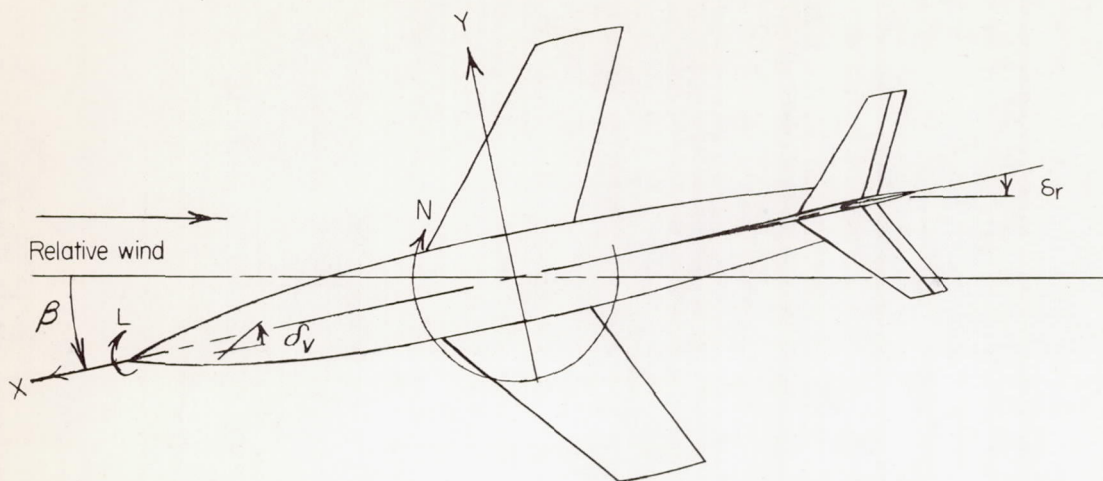
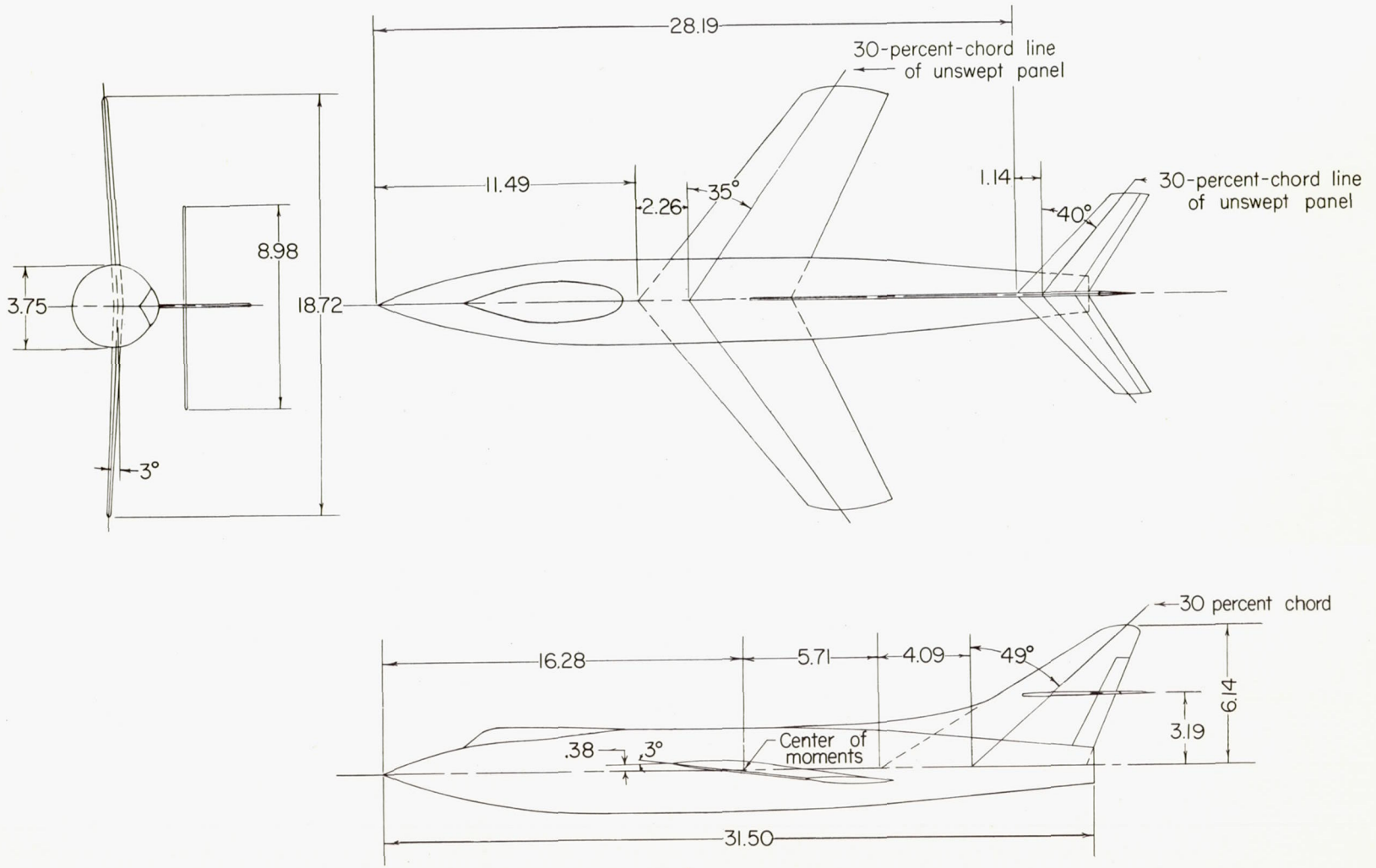


Figure 1.- System of stability axes. Arrows indicate positive values.

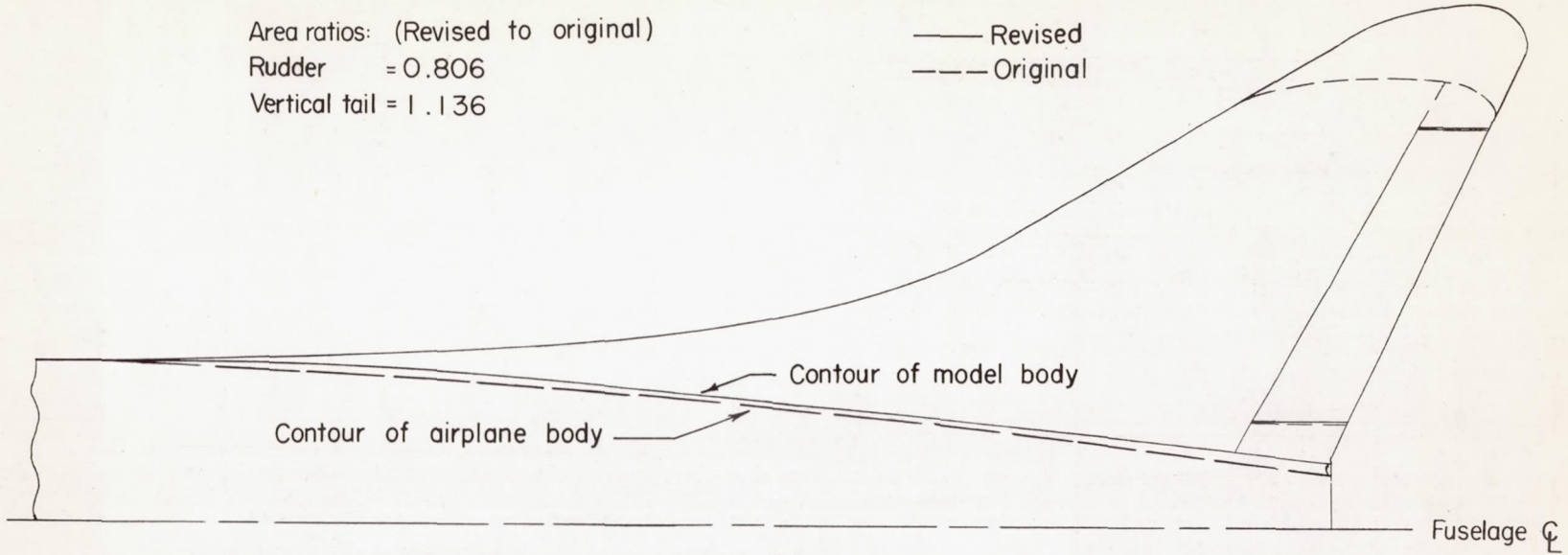


(a) Three-view drawing of complete configuration.

Figure 2.- Details of model. All dimensions are in inches.

Area ratios: (Revised to original)
Rudder = 0.806
Vertical tail = 1.136

— Revised
- - - Original



(b) Vertical-tail configurations of revised and original models.
Vertical-tail area ratio based on exposed area.

Figure 2.- Concluded.

CONFIDENTIAL

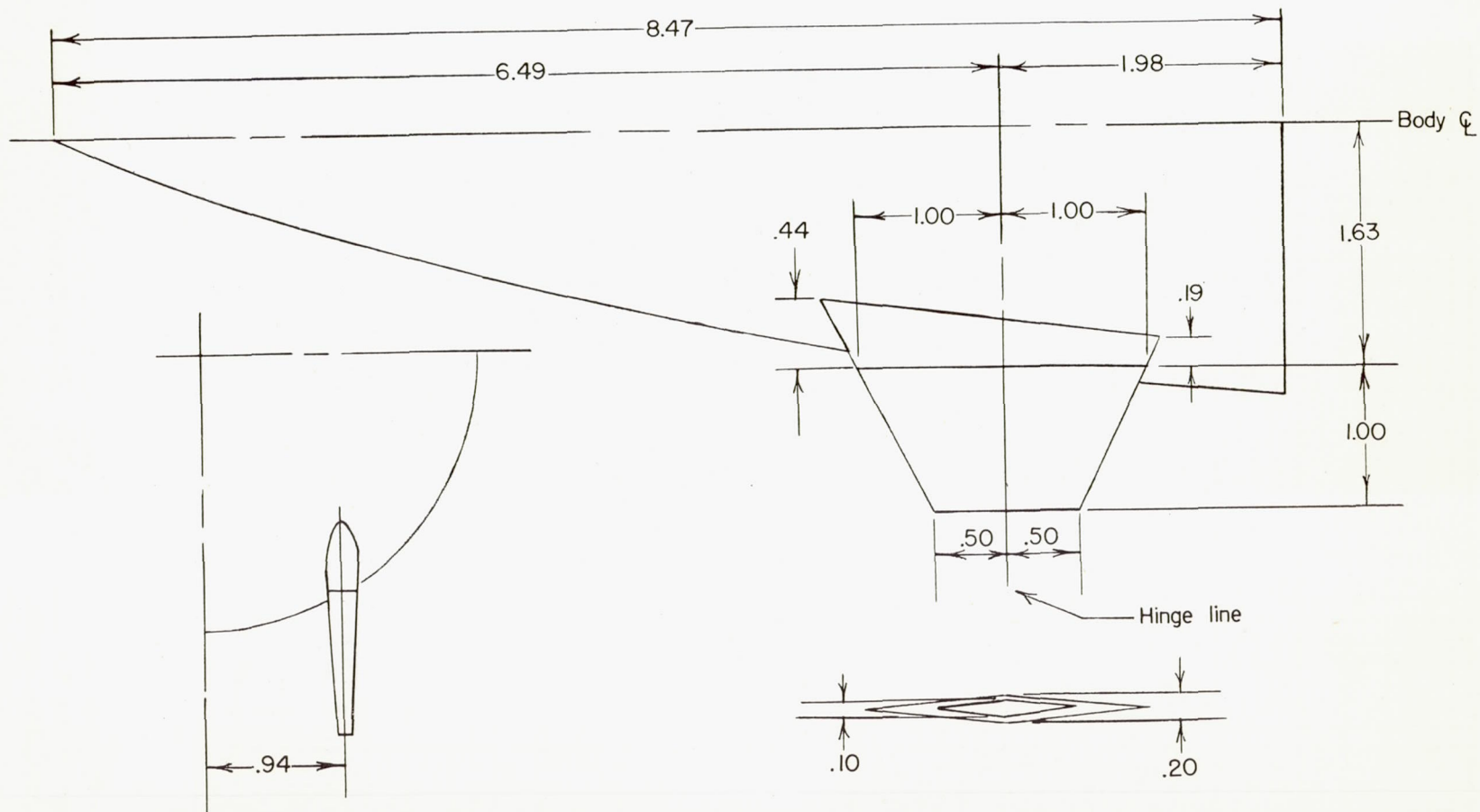


Figure 3.- Details of yaw-damper vane. All dimensions are in inches.

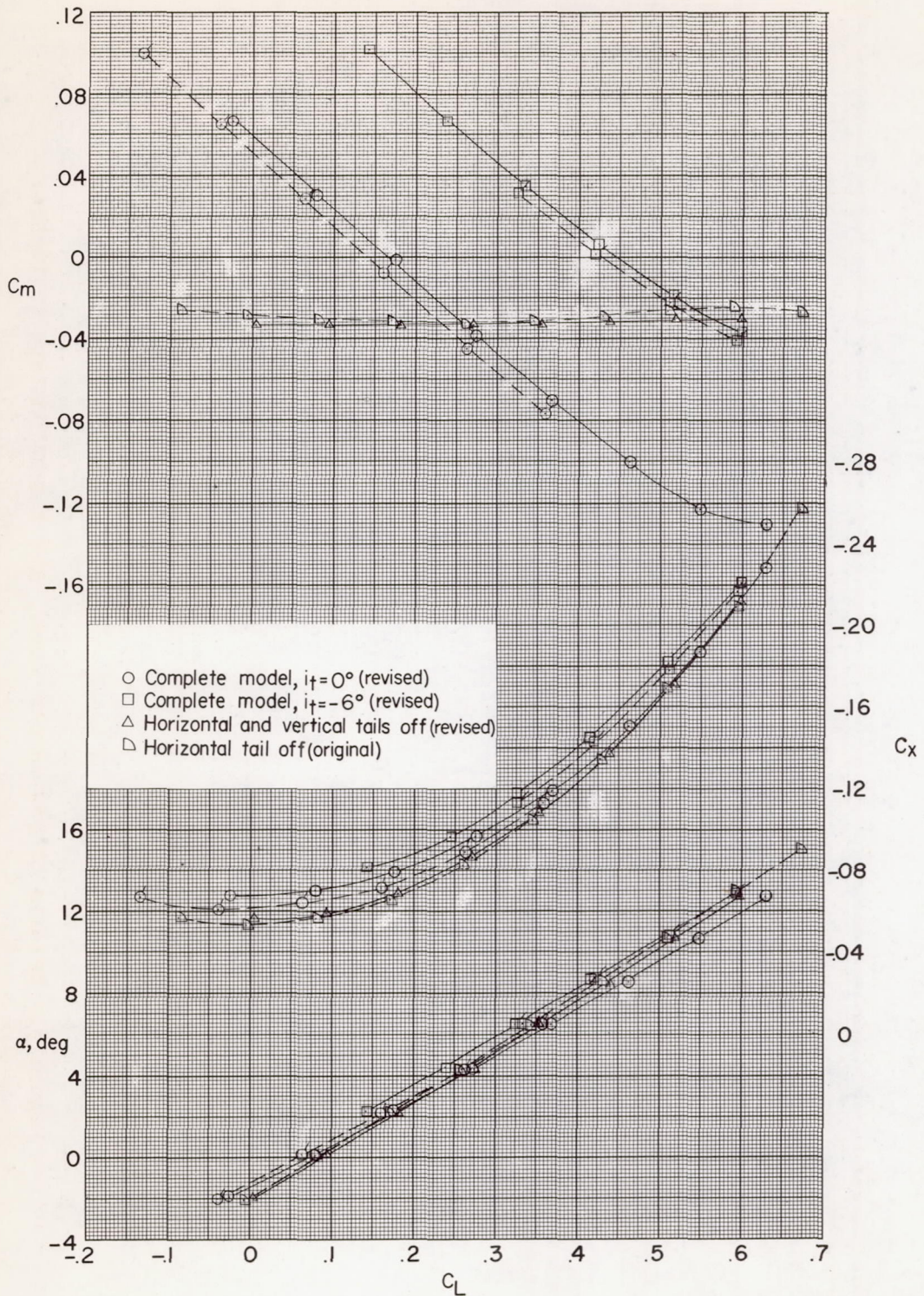


Figure 4.- Effects of canopy and revised vertical tail on the aerodynamic characteristics in pitch, $\beta = 0^\circ$. Flagged symbols and dashed lines are for original model (ref. 2).

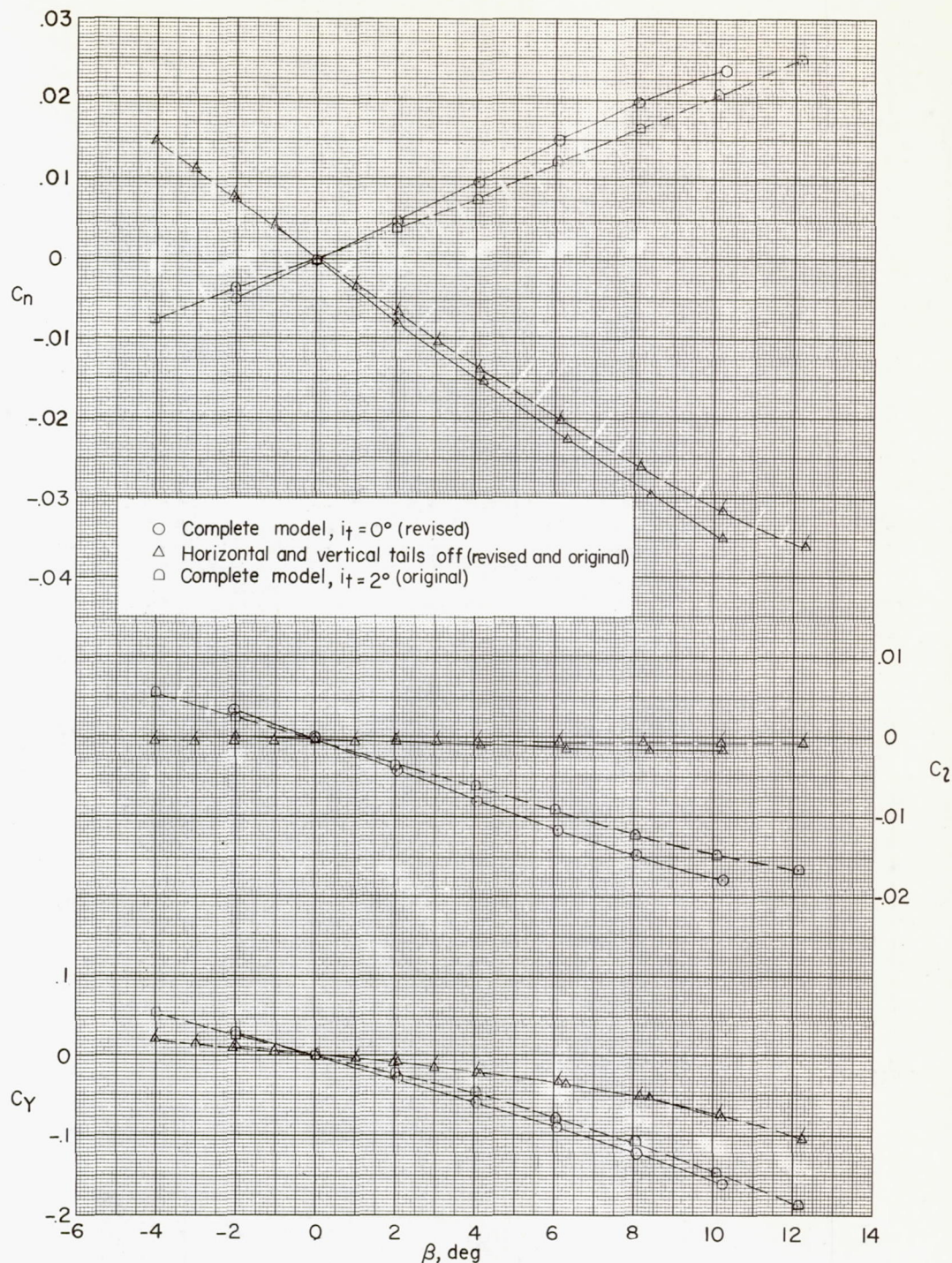
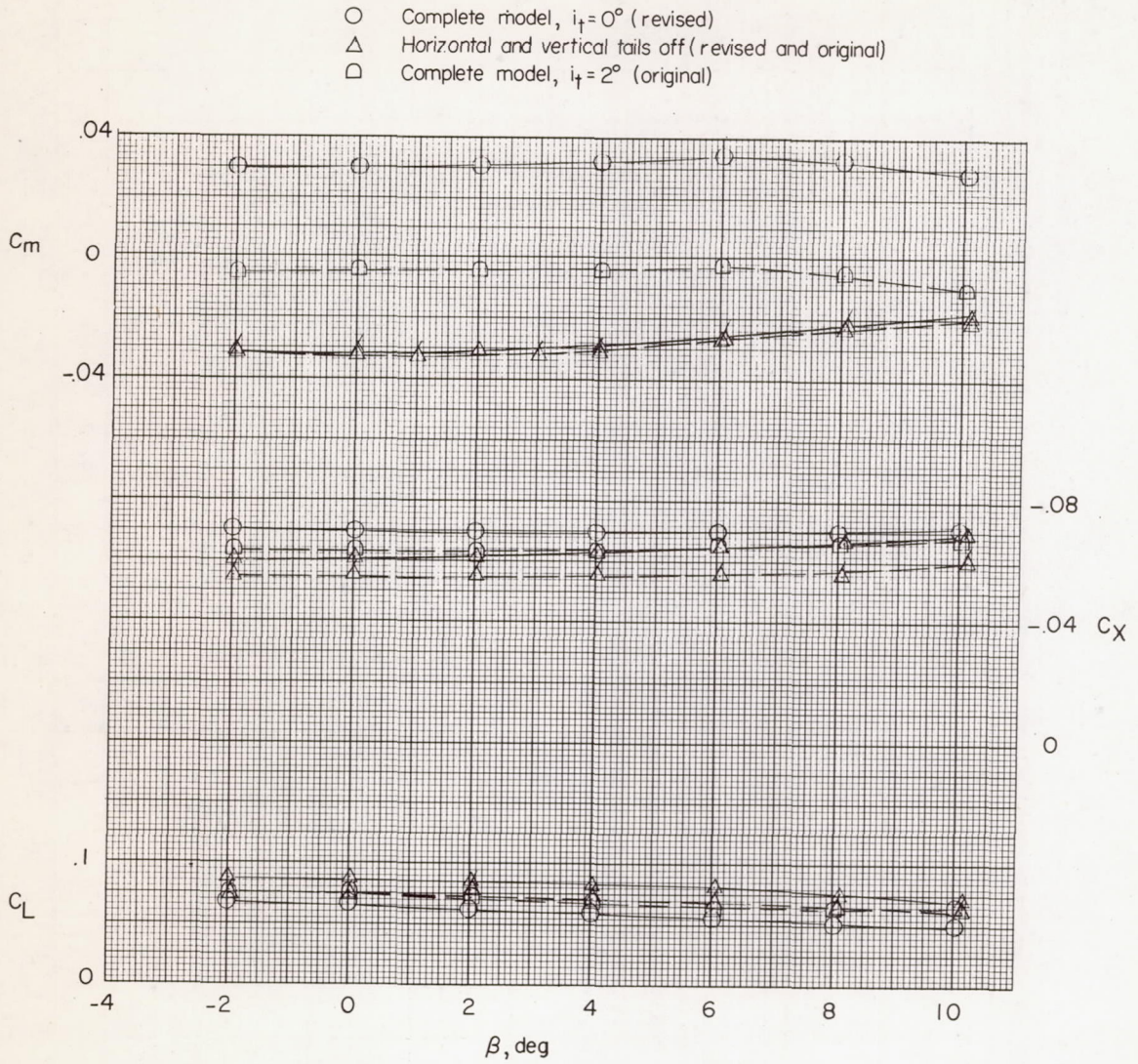
(a) C_n , C_l , and C_y against β .

Figure 5.- Effects of canopy and revised vertical tail on the aerodynamic characteristics in sideslip, $\alpha = 0^\circ$. Flagged symbols and dashed lines are for original model (ref. 2).



(b) C_L , C_X , and C_m against β .

Figure 5.- Concluded.

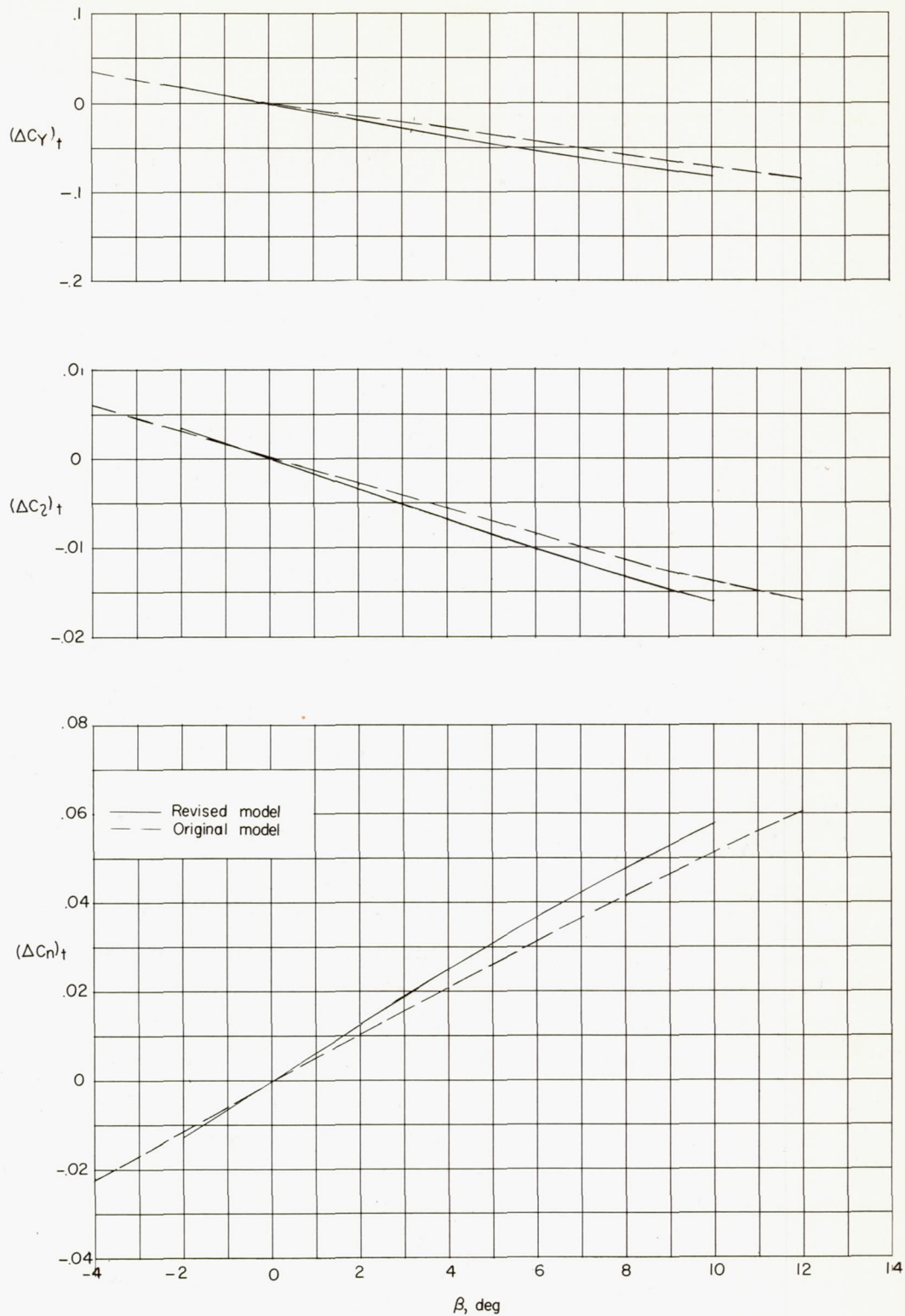


Figure 6.- Effect of canopy and revised vertical tail on $(\Delta C_Y)_t$, $(\Delta C_l)_t$, and $(\Delta C_n)_t$. $\alpha = 0^\circ$.

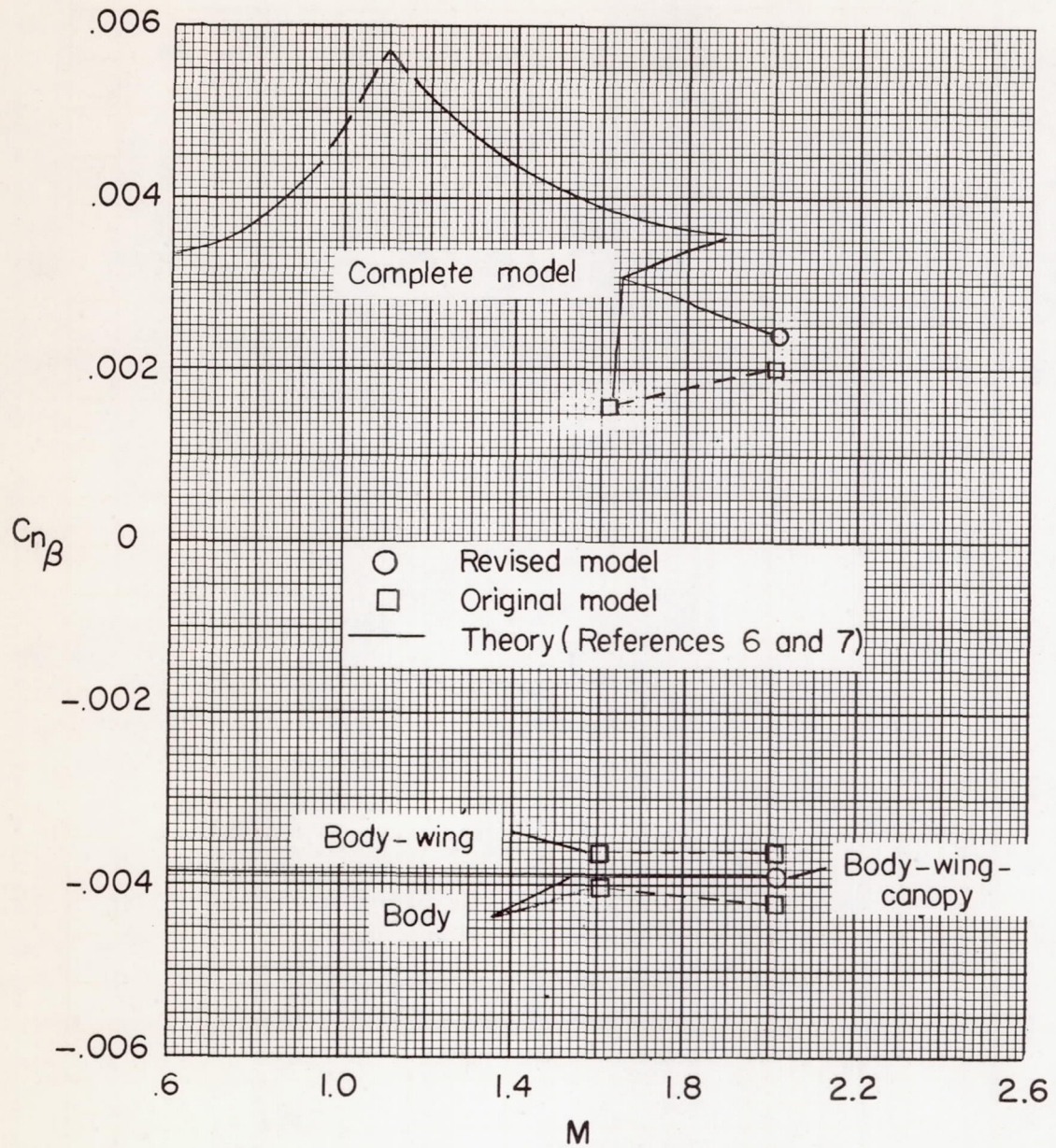
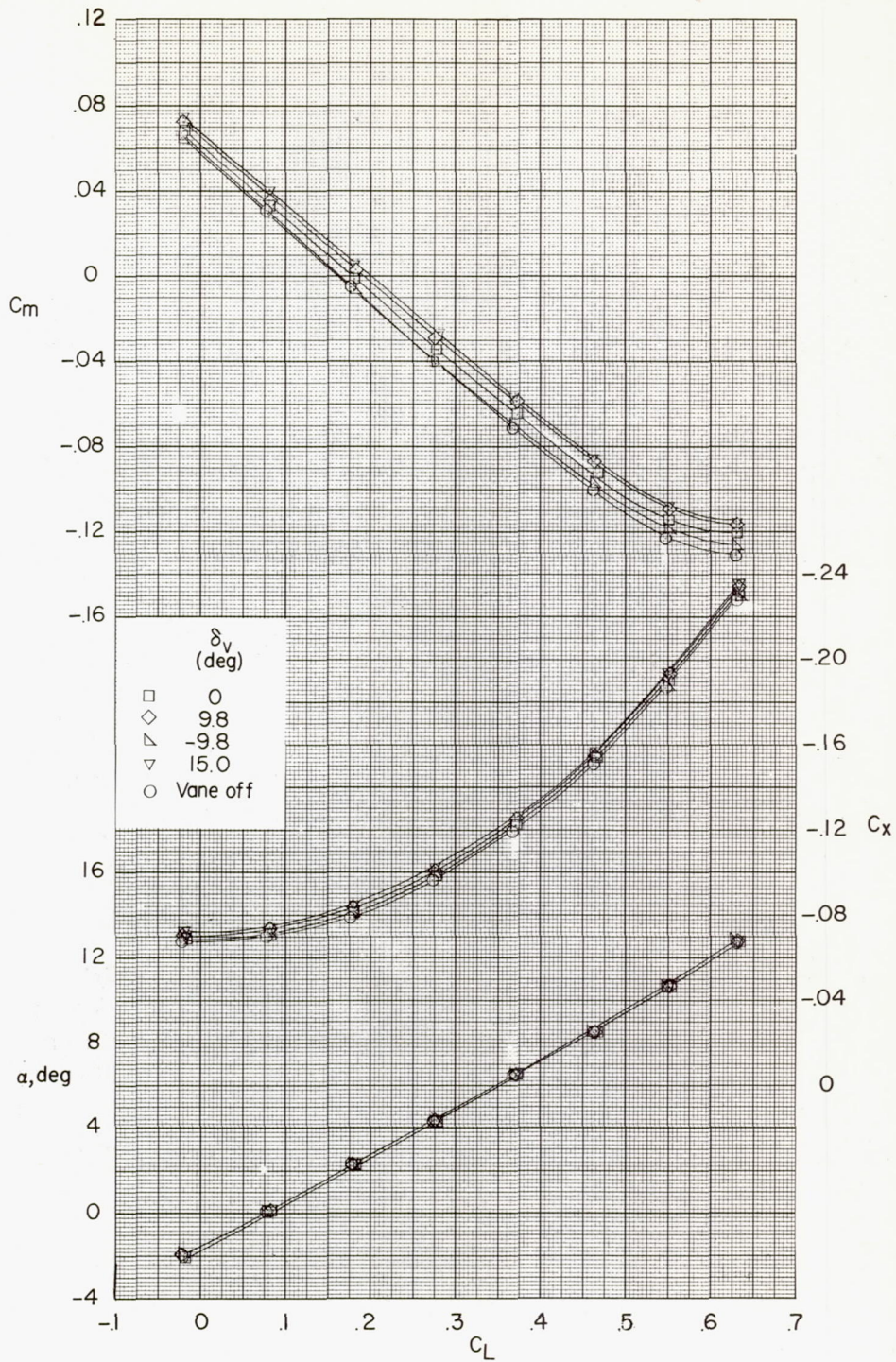
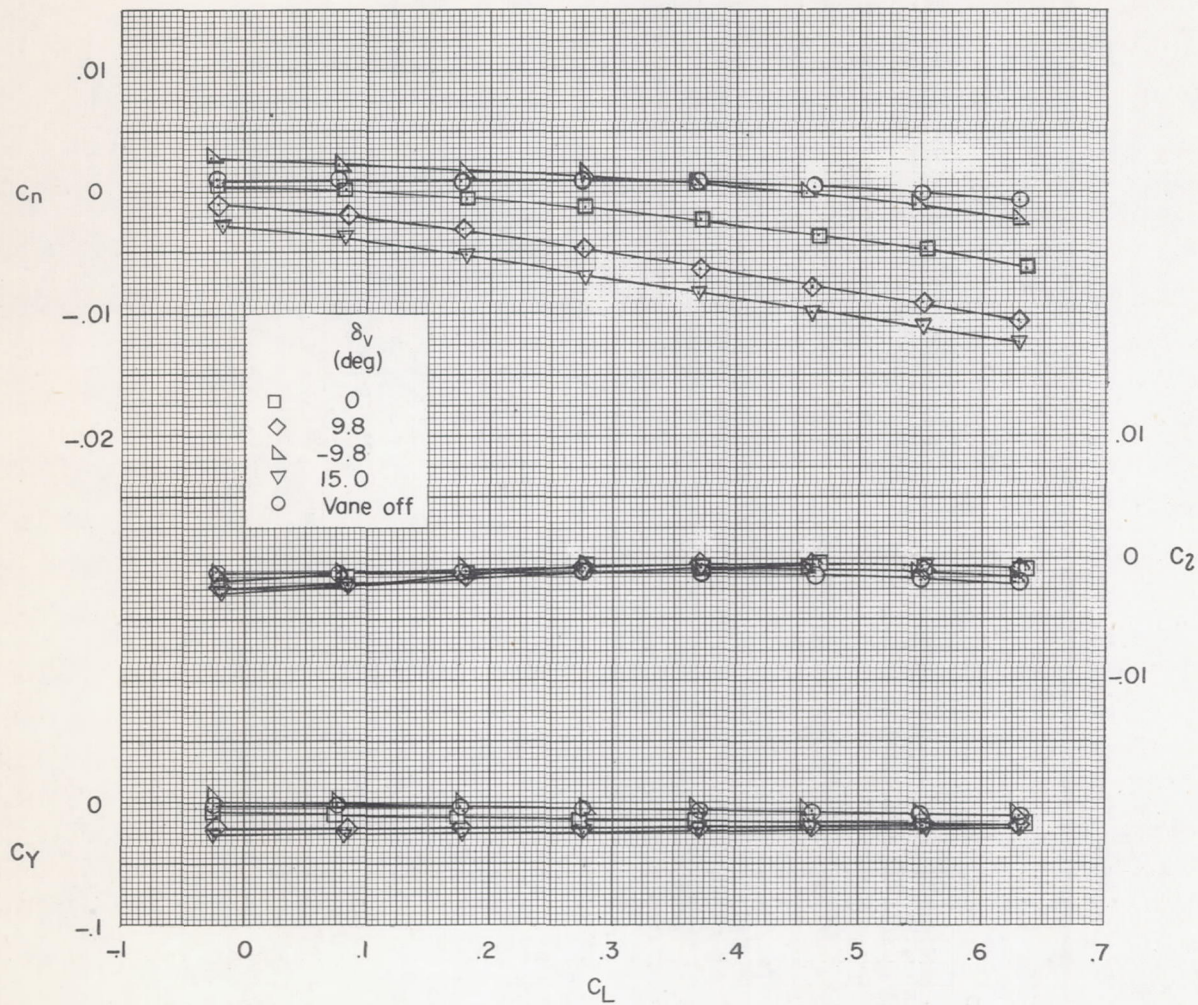


Figure 7.- Variation of $C_{n\beta}$ with M . $\alpha = 0^\circ$.



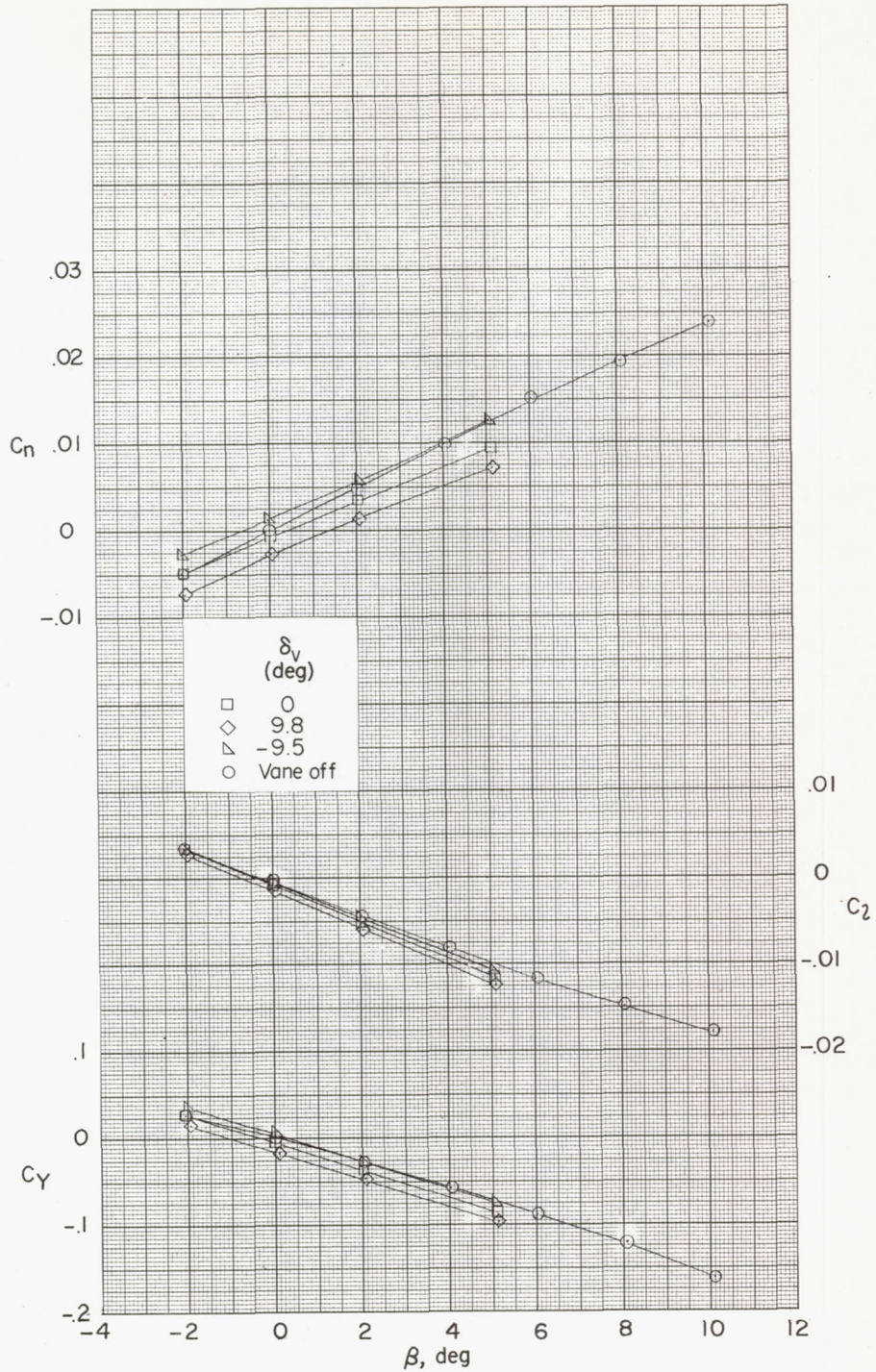
(a) C_m , C_x , and α against C_L .

Figure 8.- Effect of yaw-damper-vane deflection on the aerodynamic characteristics in pitch. Complete model; $\beta = 0^\circ$; $i_t = 0^\circ$.



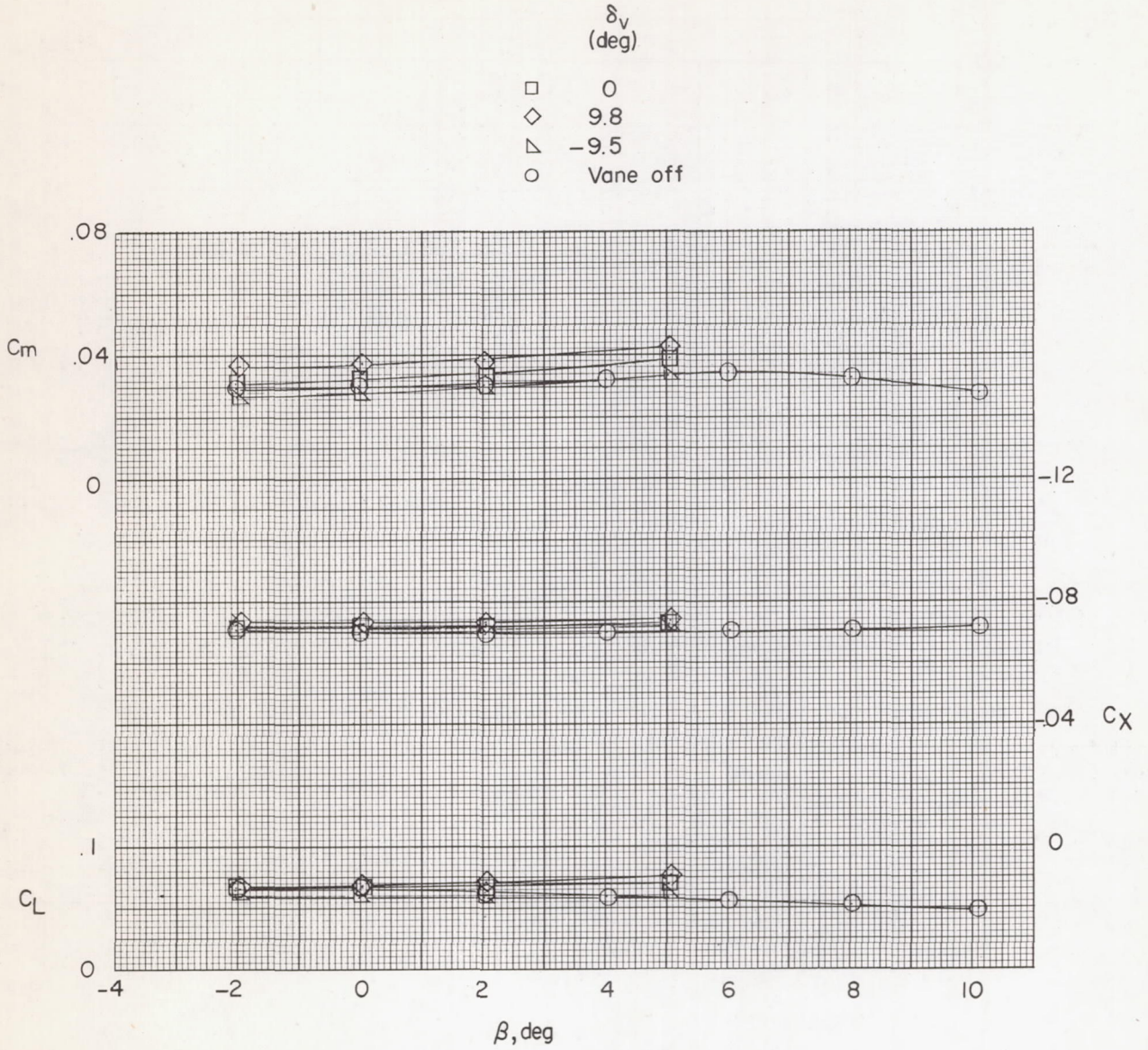
(b) C_n , C_l , and C_y against C_L .

Figure 8.- Concluded.



(a) C_n , C_l , and C_y against β .

Figure 9.- Effect of yaw-damper-vane deflection on the aerodynamic characteristics in sideslip. Complete model; $\alpha = 0^\circ$; $i_t = 0^\circ$.



(b) C_m , C_x , and C_L against β .

Figure 9.- Concluded.

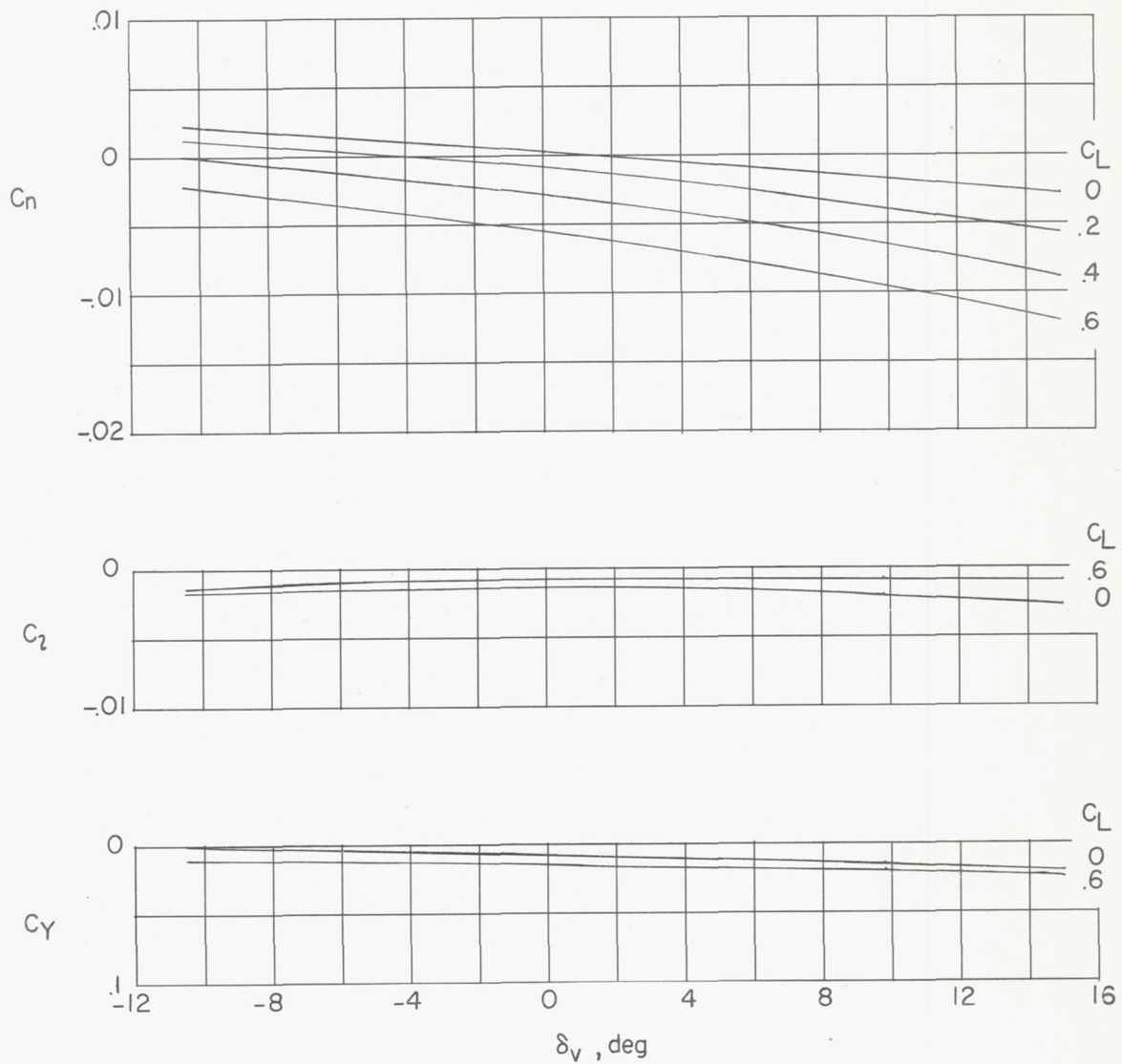
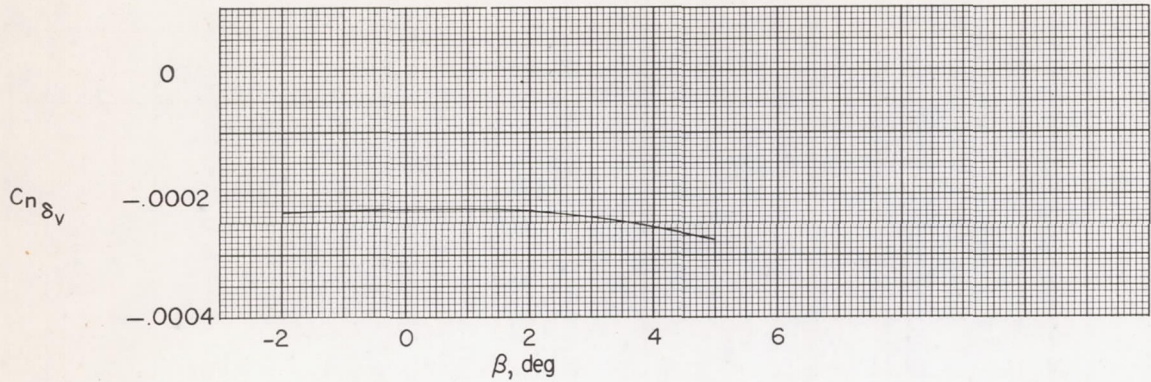
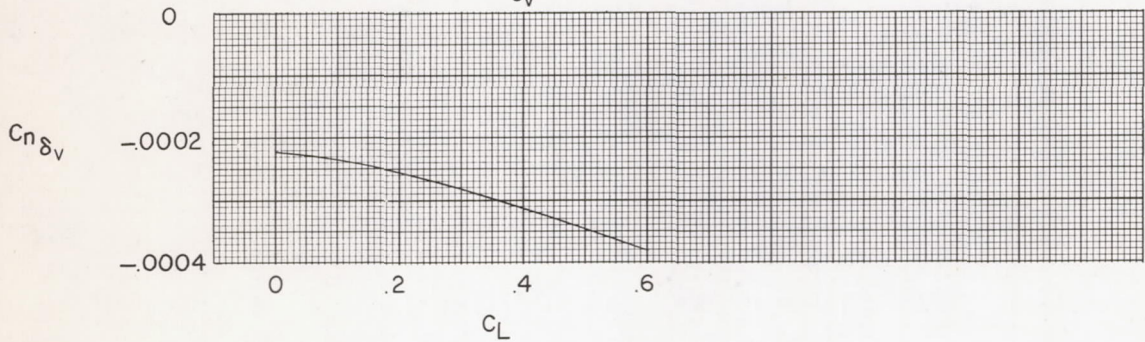


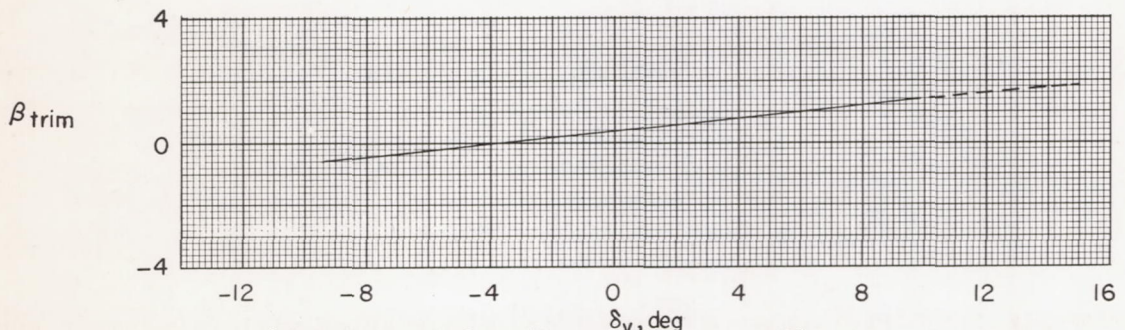
Figure 10.- Variation of lateral characteristics with yaw-damper-vane deflection for several values of lift coefficient. $\beta = 0^\circ$; $i_t = 0^\circ$.



(a) Variation of $C_{n\delta_v}$ with β , $\alpha = i_t = 0^\circ$.



(b) Variation of $C_{n\delta_v}$ with C_L , $\beta = i_t = 0^\circ$.



(c) Variation of β_{trim} ($C_n = 0$) with δ_v , $\alpha = i_t = 0^\circ$.

Figure 11.- Summary of yaw-damper-vane characteristics.

CONFIDENTIAL

CONFIDENTIAL